JOURNAL OF CATALYSIS **130**, 116–129 (1991)

Synthesis and Activity of Hydrotreating Catalysts Prepared via Promotion by Low-Valent Transition-Metal Complexes

T. R. HALBERT, T. C. HO, E. I. STIEFEL, R. R. CHIANELLI, AND M. DAAGE

Exxon Research and Engineering Co., Rt 22 East, Annandale, New Jersey 08801

Received April 16, 1990; revised January 30, 1991

A new family of hydrotreating catalysts is developed via low-temperature chemical reaction of the edge of preformed MoS_2 particles. Specifically, an "edge decoration" is achieved via reaction of MoS_2 with low-valent organometallic complexes such as $Co_2(CO)_8$. This approach is suggested by the reactivity of similar low-valent organometallics with molecular complexes whose structure contains fragments that resemble those in transition-metal sulfides. Activity tests with pure compounds and commercial feedstocks have shown that these catalysts are active for hydrodesulfurization. © 1991 Academic Press, Inc.

INTRODUCTION

Research on the nature of Co/Mo transition-metal sulfide-based hydrotreating catalysts has led to the proposal of a number of models for the active phase composition and structure. The four main types of models, as illustrated in Fig. 1, are the monolayer model (*1, 2*), the contact synergy model (*3*), the intercalation model (*4, 5*), and the edge decoration model (*6, 7*). Recent experimental advances have tended to support the idea that the catalytically active component of Co/Mo/S-based hydrodesulfurization (HDS) catalysts contains an intimate mixture of Co, Mo, and S, in keeping with either the intercalation or edge decoration model. Although many details of structure and stoichiometry remain to be determined, it is reasonably certain that homometallic phases such as Co_9S_8 and MoS_2 are of secondary catalytic importance in Co/Mo-based synergic systems.

With the above in mind, it is apparent that a primary goal of hydrotreating catalyst research should be the search for approaches that generate highly dispersed heterometallic sulfide phases (e.g., "CoMoS"), and minimize phase separation to simple binary sulfides. Two general approaches have been developed:

—Thermal decomposition of molecular transition metal/sulfur complexes, either starting from intimate (molecular level) mixtures of two or more transition metal/sulfur complexes (*8–11*), or starting from molecular complexes in which the two (or more) metals are part of the same molecular sulfur-ligated cluster at the outset (*12–16*).

—Chemical "decoration" of the edges of preformed MoS_2 particles via a chemical reaction that covalently binds the promoter metal onto the surface of the sulfide (*17, 18*).

Application of the second strategy would be aided by knowledge of the structure and reactivity of edge sites on MoS_2 particles. Although such information is being actively sought by researchers in hydrotreating catalysis, no clear picture has yet emerged. Lacking this information, we can turn to our much more extensive knowledge of Mo/S molecular clusters, and apply the successful approaches for the synthesis of heterometallic clusters to generate heterometallic phases on solid surfaces (*19*).

The first section of this paper consists of a brief discussion of our research on the

0021-9517/91 $3.00

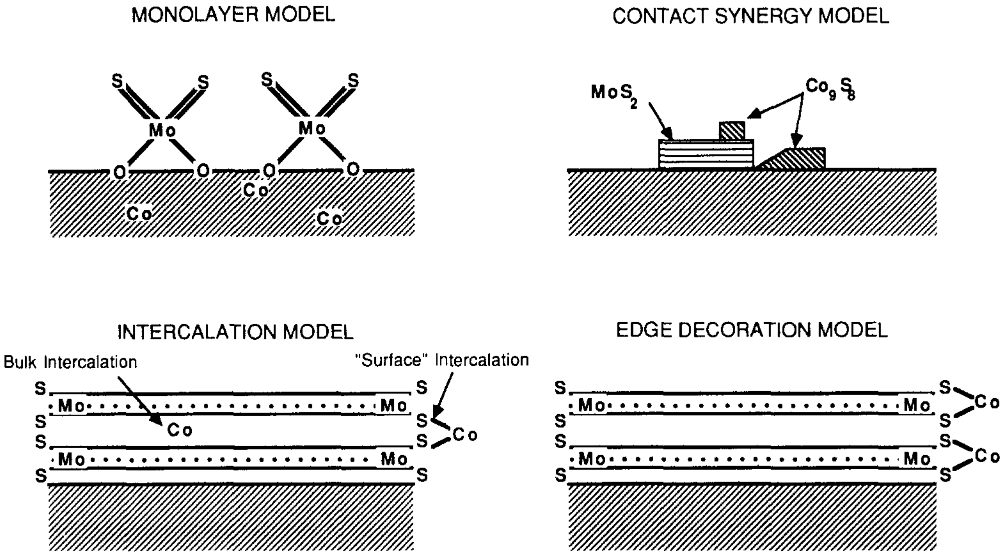

FIG. 1. Models for the promotion of molybdenum sulfide.

reactivity of known molybdenum/sulfur clusters toward cobalt-containing reagents and shows how this work guided us to the "low-valent promotion" (LVP) method of catalyst preparation. Application of the LVP method to unsupported bulk Co/Mo/S catalysts is described, including discussion of structural changes in the sulfides observed upon promotion. The LVP method was extended to supported Co/Mo/S catalysts, whose activities were tested on model feeds and real feeds for HDN (hydrodenitrogenation) and/or HDS. Finally, the use of other low-valent promoters such as Fe and Ni is described.

EXPERIMENTAL

a. General

All commercial chemicals were used as received unless otherwise noted. Dibenzothiophene (DBT) and tetrahydroquinoline were purchased from Aldrich Chemical Co. Decalin, used as a solvent, was purchased from MCB. Dicobaltoctacarbonyl ($Co_2(CO)_8$) and bis(1,5-cyclooctadiene) nickel ($Ni(COD)_2$) were purchased from Strem Chemicals and stored at −20°C under inert atmosphere. The (toluene)(1,5-cyclooctadiene) iron(0) was a kind gift of Dr. J. Bradley of our laboratory. Hexane was purchased from Burdick & Jackson and deoxygenated by bubbling with N_2 before use. Acetonitrile (Burdick & Jackson) was redistilled from CaH_2 under N_2 prior to use. Ammonium tetrathiomolybdate was purchased from SPEX Industries.

b. Molecular Catalyst Precursors

Bis(tetraethylammonium)tetrathiomolybdate $(TEA)_2MoS_4$ was prepared from $(NH_4)_2MoS_4$ by metathetical reaction with $Et_4N^+Cl^-$ in CH_3CN (*20*), and was treated with $Co_2(CO)_8$ to obtain the salt $(TEA)_3$ $Co(MoS_4)_2$, as previously described (*12*). The "thiocubane" molecule $Co_2Mo_2S_4$ $(Et_2dtc)_2(CH_3CN)_2(CO)_2$, abbreviated as CoMoCube, was prepared as described in Ref. (*21*).

c. Unsupported Catalysts

MoS_3 and MoS_2 were prepared as previously described (*22*) from thermal decomposition of $(NH_4)_2MoS_4$. Molybdenum sulfide microcrystallites (hexagonal platelets) were grown by chemical vapor transport from MoS_2 powder as previously described (*23*).

$CoMoS_4$. A solution of $(TEA)_2MoS_4$ (2 g, 4.13 mmol) in 25 ml CH_3CN was treated slowly under inert atmosphere with a solution of $Co_2(CO)_8$ (0.705 g, 2.06 mmol) in 20 ml toluene. After the vigorous CO gas evolution ended, the black precipitate was separated from the pale brown solution by filtration. The solid was dried and stored under inert atmosphere until used.

Co/MoS_3. A sample of MoS_3 (1 g, 5.2 meq Mo) was treated under inert atmosphere with a solution of $Co_2(CO)_8$ (0.09 g, 0.26 mmol) in 10 ml tetrahydrofuran. Slow CO evolution was noted. After standing overnight under N_2, the solid was filtered from the nearly colorless solution, and dried. The product was stored in inert atmosphere until used.

Co/MoS_2MC. Half a gram of microcrystalline MoS_2 was treated for 30 min with a solution of 20 mg $Co_2(CO)_8$ in 1 ml hexane, under inert atmosphere. The solid was filtered and washed two times with clean hexane, and dried under N_2.

Co/MoS_2HS. A sample of high surface area MoS_2 (1.4 g) was treated with a solution of 0.149 g $Co_2(CO)_8$ in 5 ml hexane. Vigorous CO bubbling was observed, and the solution became pale brown within several minutes. After 30 min, the solid was filtered and dried under N_2. Anal. Found: Mo, 57.5%; Co, 3.2%; S, 37.9%; C, 1.4%.

d. Unpromoted Supported Catalysts

Alumina supports were calcined for 5 h at 500°C prior to impregnation. Molybdenum sulfide species were prepared on the catalyst supports in one of two ways:, by impregnation with bis(tetrabutylammonium)tetrathiomolybdate $(TBA)_2MoS_4$ in MeOH (*24*) and drying in vacuum, or by aqueous impregnation with ammonium heptamolybdate followed by calcination and H_2/H_2S sulfiding at 400°C. Catalysts prepared by the former method are designated MoTBA/AlL, where AlL denotes use of a large-pore alumina (mean pore diameter = 110 Å, 160 m^2/g). Catalysts prepared by the latter method are designated MoS/AlL and MoS/AlS, where AlL is as above, and AlS is a small-pore alumina (mean pore diameter = 60 Å, 250 m^2/g).

e. Promotion of Supported Catalysts

A list of final promoted catalysts used is given in Table 1, along with general information about each catalyst, including the unpromoted sample from which it was prepared (base catalyst), promoter, final Mo content, and promoter ratio. Details of representative synthetic procedures are given below.

Co/MoTBA/AlL. A sample of MoTBA/AlL (5 g) was stirred in 20 ml hexane under inert atmosphere. A solution of $Co_2(CO)_8$ (0.17 g) in 10 ml hexane was added. Rapid CO evolution was observed, the solid changed from orange to green-black, and the solution became nearly colorless within several minutes. After cessation of gas evolution, the solid was filtered and dried under inert atmosphere. Promotion of the small-pore alumina sample was carried out in identical fashion.

Co/MoS/AlS-(A–K) and Co/MoS/AlL-(A–B). These samples were all prepared in an analogous fashion. The preparation of Co/MoS/AlS-A (see Table 1) is given in detail as an example: A sample of Mo/AlS-1 (3 g) was treated with a dark brown solution of $Co_2(CO)_8$ (0.232 g) in 6 ml hexane under inert atmosphere. The slurry was agitated gently until CO evolution ceased (about 5 min). After standing for an additional hour, the solid was filtered from the nearly colorless solution, and dried *in vacuo.*

CoM/MoS/AlS. A sample of MoS/AlS-2 (4 g, 1.8 mmol Mo) was treated with a solution of $[(C_6H_5)_4P]_2Co(SC_6H_5)_4$ (0.47 g, 0.4 mmol) in 25 ml acetonitrile. After stirring under inert atmosphere for 48 h, the pale green solution was filtered from the black solid. The solid was washed with acetonitrile and hexane, then dried *in vacuo.*

CoN/MoS/AlS. A sample of MoS/AlS-2 (4 g, 1.8 mmol Mo) was treated with a solution of $Co(NO_3)_2 \cdot 6H_2O$ (0.212 g, 0.85 mmol) in 10 ml acetone. Significant heating

TABLE I

Promotion of Supported Molybdenum Sulfide Catalysts

Catalyst designation	Catalyst base	Promotor	% Mo, ILF[a]	P/(P + Mo)[b]
Co/MoTBA/AlL	MoTBA/AlL	$Co_2(CO)_8$	8.50	0.25
Co/MoS/AlS-A	MoS/AlS-1	$Co_2(CO)_8$	9.44	0.35
Co/MoS/AlS-B	MoS/AlS-2	$Co_2(CO)_8$	6.44	0.39
Co/MoS/AlS-C	MoS/AlS-3	$Co_2(CO)_8$	6.00	0.41
Co/MoS/AlS-D	MoS/AlS-3	$Co_2(CO)_8$	5.97	0.31
Co/MoS/AlS-E	MoS/AlS-3	$Co_2(CO)_8$	6.00	0.31
Co/MoS/AlS-F	MoS/AlS-3	$Co_2(CO)_8$	6.00	0.24
Co/MoS/AlS-G	MoS/AlS-3	$Co_2(CO)_8$	6.00	0.24
Co/MoS/AlS-H	MoS/AlS-3	$Co_2(CO)_8$	6.00	0.18
Co/MoS/AlS-I	MoS/AlS-3	$Co_2(CO)_8$	6.00	0.08
Co/MoS/AlS-J	MoS/AlS-4	$Co_2(CO)_8$	9.32	0.34
Co/MoS/AlS-K	MoS/AlS-5	$Co_2(CO)_8$	13.8	0.27
Co/MoS/AlL-A	MoS/AlL-1	$Co_2(CO)_8$	9.50	0.20
Co/MoS/AlL-B	MoS/AlL-3	$Co_2(CO)_8$	3.10	0.13
CoM/MoS/AlS	MoS/AlS-2	$Co(S\Phi)_4^{2-}$	7.00	0.11
CoN/MoS/AlS	MoS/AlS-2	$Co(NO_3)_2$	6.00	0.32
Fe/MoS/AlS-1	MoS/AlS-3	Fe(COD)(tol)	6.00	0.33
Fe/MoS/AlS-2	MoS/AlS-1	$Fe(CO)_5$	9.44	
Ni/MoS/AlS-1	MoS/AlS-2	$Ni(COD)_2$	6.04	0.32
Ni/MoS/AlS-2	MoS/AlS-2	$Ni(P\Phi_3)_2(O)_2$	6.01	0.20

[a] Ignition loss free basis.
[b] Atomic ratio.

of the sample occurred. Solvent was removed from the sample *in vacuo*, and the dry black solid used directly in the activity test.

Fe/MoS/AlS-1. A sample of MoS/AlS-3 (4 g, 1.8 mmol Mo) was brought out of the drybox in a Schlenk flask closed with a serum cap. A dark brown solution of Fe(1,5-cyclooctadiene)(toluene) (0.27 g, 1.04 mmol) in 7 ml hexane was added via a cannula under inert atmosphere. After standing for half an hour, the solid was washed with hexane. The washing was clear. The solid was dried *in vacuo* and stored under inert atmosphere until used.

Fe/MoS/AlS-2. A sample of MoS/Al-1 (3 g, 3 mmol Mo) was suspended in 15 ml degassed toluene by vigorous stirring. Neat $Fe(CO)_5$ was added (136 ml, 1 mmol) via syringe. No evolution of CO was observed. The slurry was heated gradually, until CO evolution began (60–70°C). When gas evolution ceased (about 10 min), the solution was cooled to room temperature, filtered under inert atmosphere, and the resulting black solid dried *in vacuo*. Some iron was lost as a result of metal mirror formation on the walls of the flask.

Ni/MoS/AlS-1. Bis(1,5-cyclooctadiene) Ni^0 (0.275 g, 1 mmol) was dissolved in 15 ml hexane under inert atmosphere. The yellow slurry began to darken before dissolution was complete, so the mixture was added quickly to a sample of MoS/AlS-2 (4 g, 1.8 mmol Mo). The hexane solution turned clear immediately. After 30 min, the mixture was filtered, washed with 5 ml hexane twice, and the black solid dried *in vacuo*.

Ni/MoS/AlS-2. A slurry containing $(Ph_3P)_2Ni^0(CO)_2$ (0.64 g, 1 mmol) in 30 ml toluene was added under inert atmosphere to a sample of MoS/AlS-2 (4 g, 1.8 mmol Mo). Very slow gas evolution was observed. After stirring for 48 h, the mixture was filtered, and the black solid washed with 10 ml toluene three times to remove any unreacted

Ni complex. The solid was then dried *in vacuo*, and stored under inert atmosphere.

f. Reference Catalysts

Two commercial catalysts, KF840 (Ketjen) and HCD (American Cyanamid), were tested to provide the base case. The nominal metal compositions of these catalysts are: KF840, 13% MoO_3 and 3.1% NiO supported on γ-alumina; HCD, 18%MoO_3 and 3.5% NiO supported on γ-alumina. These catalysts were sulfided with 10% H_2S in H_2 at 360°C for 1 h.

g. Activity Tests

Model-feed reactions. The HDS and HDN activity evaluations were carried out in a modified Carberry type autoclave designed to allow a constant hydrogen flow. In order to avoid the loss of solvent and low boiling point products, a water-cooled condensor, which recycled the condensate back to the vessel, was added at the outlet of the reactor. The reaction conditions were:

0.5 to 4.0 g catalyst
100 cm^3/min (room temperature) H_2
3150 kPa hydrogen pressure
100 cm^3 liquid feed
7 h maximum contact time
350°C

Runs were conducted using two different feeds. For HDS evaluations, the feed consisted of 5 wt% dibenzothiophene dissolved in decalin. For HDN evaluations, levels of HDN and HDS were measured under competitive conditions using the above DBT/decalin mixture with 0.8 wt% N added as 1,2,3,4-tetrahydroquinoline (1,4-THQ). Product analyses were performed on an HP 5880 gas chromatograph equipped with a flame ionization detector. A 75% OV-1/25% Superox 20M capillary column (50 m × 0.25 mm) was used with a temperature ramp between 160 and 300°C (heating rate 20°C/min). In all experiments the conversion levels were maintained below 50%.

For the desulfurization of DBT, Langmuir–Hinshelwood kinetics have widely been reported (*25*, *26*).

$$r_{\mathrm{HDS}} = \bar{k}_{\mathrm{S}} \frac{K_{\mathrm{DBT}}[\mathrm{DBT}]}{(1 + K_{\mathrm{DBT}}[\mathrm{DBT}] + K_{\mathrm{H_2S}}[\mathrm{H_2S}])} \times \frac{K_{\mathrm{H}}P_{\mathrm{H}}}{(1 + K_{\mathrm{H}}P_{\mathrm{H}})}. \quad (1)$$

Under our experimental conditions, the kinetic equation can be simplified for the following reasons:

—The hydrogen pressure term is constant and can be included in the rate constant.

—The inhibition due to H_2S is not significant because of the constant hydrogen sweeping.

—The unity in the denominator can also be neglected because of the large excess of DBT in the reactor and the low conversion levels at which the samples were collected.

Based on the above assumptions Eq. (1) can be simplified to

$$r_{\mathrm{HDS}} \approx k_{\mathrm{S}} \frac{K_{\mathrm{DBT}}[\mathrm{DBT}]}{(1 + K_{\mathrm{DBT}}[\mathrm{DBT}])} \approx k_{\mathrm{S}}; \quad (2)$$

i.e., the rate constant can be evaluated from the slope of the concentration versus time plot. Indeed a linear plot was always observed for each of the catalysts tested.

Similarly, HDN activities were based on zero-order rate constant for the appearance of hydrocarbons, i.e., propylbenzene, propylcyclohexene, and propylcyclohexane (*27*).

$$r_{\mathrm{HDN}} = k_{\mathrm{N}} \frac{K_{\mathrm{N}}[\mathrm{N}]}{(1 + K_{\mathrm{DBT}}[\mathrm{DBT}] + K_{\mathrm{N}}[\mathrm{N}])} \approx k_{\mathrm{N}}. \quad (3)$$

In Eq. (3), we have assumed that the adsorption of DBT is much smaller than that of N-containing compounds.

For HDS in the presence of N-containing molecules, the kinetics of desulfurization should be first order in DBT concentration due to the N inhibition. However, in all cases the conversion levels were very low

(<5%) and the use of a zero-order kinetics is adequate. This is shown as follows:

$$r_{\mathrm{HDS}} = k_{\mathrm{S}} \frac{K_{\mathrm{DBT}}[\mathrm{DBT}]}{(1 + K_{\mathrm{DBT}}[\mathrm{DBT}] + K_{\mathrm{N}}[\mathrm{N}])} \approx k_{\mathrm{S}} \frac{K_{\mathrm{DBT}}[\mathrm{DBT}]}{K_{\mathrm{N}}[\mathrm{N}]} \approx k'_{\mathrm{S}}. \quad (4)$$

Real-feed tests: Gas oil. The test unit consisted of four reactor trains, each having a catalyst charge of 20 cc. Each reactor was heated by immersion in a common sand bath. Feed was pumped in upflow to the catalyst bed after a preheating line, and hydrogen flow was concurrent with the liquid feed. Evaluation runs were typically made for a week at 1.0 LHSV (liquid hourly space velocity), 360°C, 7700 kPa, and 5000 SCF/B pure hydrogen gas treat rate. Samples were taken for analysis of sulfur and nitrogen contents after 24 h and at 24-h intervals thereafter, until analyses demonstrated that the system was lined out. No attempt was made in this work to investigate long-term activity maintenance. The nominal feed properties are: sulfur, 1.55 wt%; nitrogen, 0.53 wt%. Sulfur analysis was carried out by X-ray fluorescence, using a Princeton Gamma-Tech Model 100 analyzer with a ^{55}Fe radioactive source. Nitrogen analysis was done by the Antek combustion method, which utilizes chemiluminescent detection of nitric oxide. Overall apparent activities were evaluated on the basis of catalyst volume using an apparent second-order kinetics for HDS and a first-order kinetics for HDN (*28*). Specifically,

$$\text{HDN} \quad k_{\mathrm{N}} = \mathrm{LHSV} \cdot \ln \frac{\mathrm{N_F}}{\mathrm{N_P}} \quad (5)$$

$$\text{HDS} \quad k_{\mathrm{S}} = \mathrm{LHSV} \cdot \left[\frac{1}{\mathrm{S_P}} - \frac{1}{\mathrm{S_F}}\right], \quad (6)$$

where k is the apparent rate constant, $\mathrm{N_F}$ and $\mathrm{S_F}$, respectively, the nitrogen and sulfur contents of the feed, $\mathrm{N_P}$ and $\mathrm{S_P}$, respectively the nitrogen and sulfur contents of the product. The selectivity for HDS, $\mathrm{S_{HDS}}$, can be calculated by taking the ratio of k_{S} to k_{N}.

Real-feed tests: Cycle oil. Evaluations of catalyst activity for hydrotreating of a heavy catalytic cycle oil (HCCO) were carried out in an automated, continuous stirred tank reactor (CSTR) unit consisting of a 1-liter autoclave, calibrated feed burette, pump, gas–liquid separator, and product liquid collector. The HCCO feed contains 0.82 wt% sulfur and 0.11 wt% nitrogen. Twenty cc of catalyst was charged in a stainless-steel basket, which was placed inside the autoclave. The test conditions were 325°C, 3150 kPa, 3000 SCF/B H_2, and 1.0 LHSV. The stirring rate was set at 1500 rpm to ensure the absence of mass transfer effects. The activities for HDN and HDS were calculated in terms of 0.5th- and 1.5th-order kinetics, respectively:

$$\text{HDN} \quad k_{\mathrm{N}} = \mathrm{LHSV} \cdot \frac{\mathrm{N_F} - \mathrm{N_P}}{\mathrm{N_P^{0.5}}} \quad (7)$$

$$\text{HDS} \quad k_{\mathrm{S}} = \mathrm{LHSV} \cdot \frac{\mathrm{S_F} - \mathrm{S_P}}{\mathrm{S_P^{1.5}}} \quad (8)$$

The choice of kinetic treatment was based on the observation of first-order HDN and second-order HDS kinetics in the tubular reactor and the fact that the apparent reaction order for heteroatom removal in a tubular reactor is generally higher than that in the CSTR by 0.5 (*29*). This phenomenon has been interpreted as arising from a wide spread in reactivity of the individual organic sulfur and nitrogen species. It should be noted that the apparent heteroatom removal kinetics represents an averaging over a reactivity spectrum and this average is of necessity a different one in reactors with different mixing characteristics.

RESULTS AND DISCUSSION

Co/Mo/S Clusters and the Low-Valent Promotion Concept

As described in the Introduction, one goal of our recent research on HDS/HDN catalysts has been the preparation of molecular catalyst precursors in which the primary catalytic metal, promoter metal, and sulfur are intimately mixed at the molecular level in a

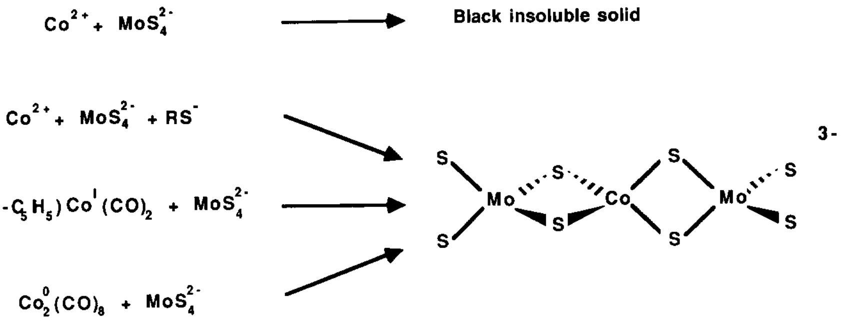

FIG. 2. Synthesis and structure of cobalt bisthiomolybdate.

single precursor (*8–16*). Our earliest attempts to achieve this goal focused on salts such as $[Co(ethylenediamine)_3]^{2+}$ $[MoS_4]^{2-}$ (*8*). Here, although the Co and the Mo are not connected by any covalent bonding network, the results of activity tests were very promising. It is also interesting to extend this series to compounds in which the Co and Mo are covalently bound, rather than located in separate anion and cation portions of a salt. We therefore set out to synthesize simple heteronuclear Co/Mo/S complexes.

The binary anion MoS_4^{2-} is certainly the simplest molecular Mo/S starting material. As early as 1971, Müller had recognized the potential of this anion as a chelating ligand in formation of heterometallic clusters of the form $M(MoS_4)_2^{2-}$. Between 1971 and 1983, a number of such complexes were reported (*30*), including those with M=Zn, Ni, Pd, Pt, and Mo=S. Unfortunately, despite the efforts of a number of researchers, the dianionic complexes with M=Co or Fe could not be prepared. Subsequent reports of the stablity of the trianion $Fe(MoS_4)_2^{3-}$, however, led to our synthesis and characterization (*12*, *13*) of the trianion $Co(MoS_4)_2^{3-}$, as shown in Fig. 2. Success in this synthetic effort was based on recognition of the need to attain low-valent Co^I in the stable trianion. This could be achieved either by starting with a low-valent cobalt precursor (e.g., $C_5H_5Co(CO)_2$ or $Co_2(CO)_8$) or by using a Co^{II} or Co^{III} complexes in the presence of a reducing agent.

More recent work has shown that the reaction of low-valent Co species with dinuclear Mo/S complexes can also be used to form larger Co/Mo/S clusters. An illustration of this is the formation of the $Co_2Mo_2S_4$ "thiocubane" complex (abbreviated CoMoCube) shown in Fig. 3 from the reaction of $Co_2(CO)_8$ with $Mo_2S_4[(C_2H_5)_2NCS_2]_3$ (*21*).

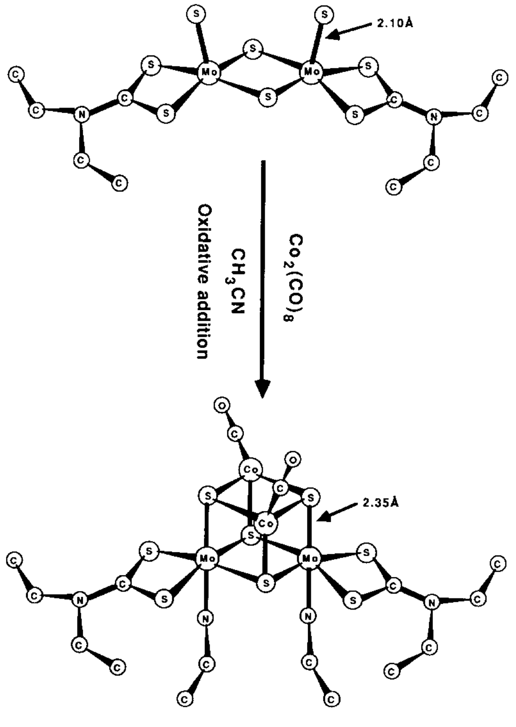

FIG. 3. Synthesis and structure of the "CoMoS" cube.

TABLE 2

Activity of Catalyst Derived from Molecular Precursors for DBT HDS

Molecular precursor	Rate × 10^{16} [a]		
	HDS	BP[b]	CHB[b]
$(TBA)_2MoS_4$	40.8	23.4	17.4
$Co(en)_3MoS_4$	149	107	41.4
$(TEA)_3Co(MoS_4)_2$	245	203	41.4
CoMoCube	374	345	29.0

Note. Reaction conditions: Batch reactor, 5 wt% DBT/decalin, 1 g catalyst, 350°C.

[a] Molecules · sec^{-1} · (g eq metal sulfide recovered)$^{-1}$.

[b] BP, biphenyl; CHB, cyclohexylbenzene.

When decomposed *in situ*, the two molecular catalyst precursors $Co(MoS_4)_2^{3-}$ and CoMoCube form active HDS catalysts. The resulting solids have BET surface areas ranging from 10 to 30 m^2/g and have an X-ray diffraction similar to that of a mixture of poorly crystalline MoS_2 and Co_9S_8. Table 2 compares the results obtained by using the molecular precursors with selected results for other catalysts and catalyst precursors. It is clear that the CoMoCube precursor shows improved catalytic activity. The covalent bonding of Co, Mo, and S in a precursor cluster apparently facilitates the formation of an active Co-promoted Mo/S phase. The connection between such heterometallic cluster complexes and the HDS catalytic phase is further strengthened by available Mössbauer emission data which suggest that $Co(MoS_4)_2^{3-}$ may have electronic and structural features similar to those of the "CoMoS" active phase proposed by Topsøe and coworkers (*31*).

Having shown that low-valent Co species such as $Co_2(CO)_8$ form covalent complexes with a variety of molecular Mo/S complexes, we suspected that low-valent Co (and other metal) complexes might react with the surface of Mo/S solids, and with Mo/S species on supports such as alumina, to form similar HDS active Co/Mo/S phases. The following sections demonstrate that this is indeed the case, and that the procedure which we now refer to as the LVP method is general and effective.

$Co_2(CO)_8$ Promotion of Bulk Mo/S Solids

Three different types of Mo/S solids have been treated with $Co_2(CO)_8$ and studied in the model HDS reaction. The first is MoS_3, an amorphous solid which has been shown to have a structure in which chains of Mo atoms are bridged by S_2^{2-} and S^{2-} groups (*32*). Individual chains are then "cross linked" by interchain Mo–S bonds. A likely mode of reaction involves oxidative addition of the low-valent metal species to the disulfide ligands on molybdenum. The limiting Co/Mo ratio would then depend on the degree to which the Co reactant could contact individual reactive sites. Since the surface area of MoS_3 used is typically about 20 m^2/g, a final ratio significantly less than 1 : 1 was expected. In practice, the reaction with $Co_2(CO)_8$ is slow and in the sample used for the catalytic testing (Co/MoS_3), the final atomic ratio Co/Mo = 0.09.

The second solid investigated was microcrystalline MoS_2 prepared by vapor transport, and referred to as MoS_2MC. In crystalline MoS_2, the basal plane S atoms has been shown to be unreactive; each sulfur is bound to three Mo atoms and should show little tendency to act as a ligand to bind Co. In contrast, the edges of the MoS_2 crystallites are much more likely to contain sites where sulfur species would react and coordinate with Co as evidenced by scanning Auger of cobalt-doped single crystal of MoS_2 (*33*). This particular Co segregation on the edges is referred to as the edge decoration of MoS_2. Because MoS_2MC is composed of relatively large crystallites (1.7 μm average diameter), a low ratio of Co/Mo upon reaction with $Co_2(CO)_8$ was expected (*23*). From the Mo edge density, estimated by SEM (6.1×10^{17} sites/g), a theoretical Co/Mo atomic ratio of 1.6×10^{-4} is obtained by assuming one promoter cobalt atom per edge site. Elemental analysis showed that this ratio was indeed lower than 0.01. Also, no significant morphological changes have been observed

TABLE 3

Promotion of Bulk Molybdenum Sulfide for DBT HDS

	Unpromoted catalysts			Promoted catalysts		
	MoS_2HS	MoS_2MC	MoS_3	Co/MoS_2HS	Co/MoS_2MC	Co/MoS_3
Rate × 10^{16}[a]						
HDS	40	4.8	17	323	16.1	131.0
BP	28	4.8	10.5	240	16.1	82.0
CHB	12	—	6.5	83	—	48.8
Co/Mo[b]				0.10	<0.01	0.09
Promotion factors						
HDS				8.1	3.4	7.7
BP				8.6	3.4	7.8
CHB				6.9	—	7.5

Note. Reaction conditions: Batch reactor, 5 wt% DBT/decalin, 1 g catalyst, 350°C.

[a] Molecules · sec^{-1} · g^{-1}.

[b] Atomic ratio.

by SEM after the promotion of the microcrystallites.

The third bulk solid studied was a sample of high surface area, poorly crystalline MoS_2 referred to as MoS_2HS (200 m^2/g). Unlike the microcrystalline MoS_2MC, this sample has a relatively high edge site density (3.5×10^{18} sites/g) as estimated by using the turnover frequency previously measured for bulk MoS_2 (*23*). Not surprisingly, then, this material was found to react with significantly more $Co_2(CO)_8$, giving a final ratio Co/Mo = 0.1.

Table 3 gives the activities obtained for the desulfurization of DBT on both promoted and unpromoted bulk catalysts. As expected, the promoted materials are more active. However, no significant changes in BP/CHB (biphenyl/cyclohexylbenzene) ratio upon promotion were observed. While the promotion factors, defined as the ratio of the rate for the promoted catalyst to the rate for the unpromoted catalyst, are about the same for biphenyl and cyclohexylbenzene production on a given Mo sulfide, the promotion factor is lower for MoS_2MC when compared to MoS_3 or MoS_2HS. Since the same chemistry, namely reaction with $Co_2(CO)_8$, was used for all materials, this result suggests that the promotion factor is dependent upon the morphology of the molybdenum sulfide base. This conclusion is further supported by numerous data reported in the literature where the promotion factor was found to vary by one order of magnitude. One plausible explanation for the above observation involves possible morphological changes in the Mo sulfide catalyst, induced by Co promotion. If the Mo/S morphology was preserved during the promotion, the promotion factor should be the same for all Mo/S base catalyst morphologies. Different morphologies would simply have different sites densities, but all would be promoted to the same degree as predicted by the electronic promotion theory (*34*). However, if the Co induces morphological changes, the promotion factor will be dependent on the capacity of the particular Mo/S system to undergo such changes. On a poorly crystalline or amorphous material like MoS_2HS, structural defects in the MoS_2 layer (for example S_2 species) are very common (*23*) and are likely to react with the low-valent promoter. Such a reaction results in weakened Mo/S bonding and may induce drastic morphological changes. The observed promotion factor may be due as much to this structural change as to any electronic promotion effect of Co. A better estimate of the electronic promotion factor is found in the promotion of the MoS_2MC sample, where the high crystallinity of the MoS_2 phase resists gross morphological change because of the low concentration of structural defects (*23*). The value of 3.3, observed for MoS_2MC, is similar to the value predicted by the model and therefore represents an upper limit on the true electronic promotion factor.

$Co_2(CO)_8$ Promotion of Alumina Supported Mo/S

The extension of the LVP method to supported catalysts requires that some form of Mo/S species be preformed on the alumina support. Two type of samples were used. MoTBA/Al, which was not thermally decomposed, is believed to react like MoTBA alone, leading to the formation of supported $Co(MoS_4)_2^{3-}$ as observed in the Co/Mo/S cluster synthesis. In that particular case, addition of $Co_2(CO)_8$ was limited to the amount required to achieve a Co/(Co + Mo) atomic ratio of 0.25, but higher ratios are probably possible. Conventional supported MoS_2 catalysts (MoS/Al) were prepared up to a Co/(Co + Mo) ratio of 0.41. The high ratio obtained for supported catalysts, compared to bulk catalysts, resulted from the higher ratio of edge to basal plane (higher dispersion) and the $Co_2(CO)_8$ reaction with the alumina surface as previously observed by Schneider *et al* (*35*). In this prior work, it was observed that the low-valent cobalt can be oxidized by reaction with the alumina surface to form a carbonate. Under hydrotreating conditions, it is likely that the resulting Co^{II} will combine with Mo/S species to form a promoted phase and/or Co_9S_8 as observed in conventional preparations of supported Co/Mo/S.

Catalytic tests of the supported LVP catalysts were conducted on the model HDS feed, on the model HDS/HDN feed, and on real feeds (HCCO and gas oil). The HDS rates obtained from model HDS tests using both unpromoted and promoted alumina-supported catalysts are given in Table 4. While the two unpromoted catalysts show very similar overall HDS activities, MoTBA/AlL shows a much higher selectivity toward CHB production. This is in keeping with previous observations on supported MoTBA catalysts (*24*). Upon reaction with $Co_2(CO)_8$, relatively large promotion factors are observed for BP production (12.8 and 14.7). These promotion levels are almost twice as large as those observed with the bulk MoS_3 and MoS_2HS samples. In contrast, the promotion factors for CHB production are actually lower than those for bulk catalysts. The net result is that the supported $Co_2(CO)_8$ promoted catalysts have a high degree of selectivity toward BP production. This effect is particularly dramatic for Co/Mo/AlS, where the base MoS/AlS material already exhibited a relatively large BP/CHB selectivity.

TABLE 4

Activity of Supported Catalysts for DBT HDS

Catalyst	% Mo	Co/Mo[b]	Rate × 10^{16} [a]		
			HDS	BP	CHB
MoTBA/AlL	8.7	—	12.5	8.7	3.8
Co/MoTBA/AlL	8.5	0.25	127.0	111.0	16.0
Promotion factor			10.2	12.8	4.2
MoS/AlS-I	10.3	—	16.1	13.3	2.8
Co/Mo/AlS-A	9.4	0.35	216.0	196.0	20.0
Promotion factor			13.4	14.7	7.1

Note. Reaction conditions: Batch reactor, 5 wt% DBT/decalin, 1 g catalyst, 350°C.

[a] Molecules · sec^{-1} · g^{-1}.

[b] Atomic ratio.

The HDS and HDN activities, for a set of catalysts with varying levels of $Co_2(CO)_8$ on the same MoS/AlS (6% Mo), were measured under competitive conditions using a feed containing a mixture of DBT and 1,4-THQ. Figure 4 shows the variations in HDS and HDN activity as a function of the promoter

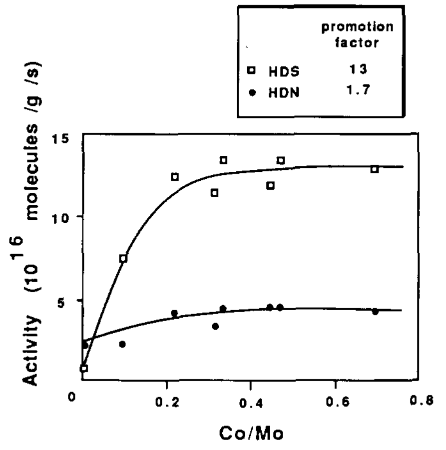

FIG. 4. Variation in HDS and HDN activities as a function of the promoter concentration (catalysts Co/MoS/AlS-C through Co/MoS/AlS-I and MoS/AlS-3).

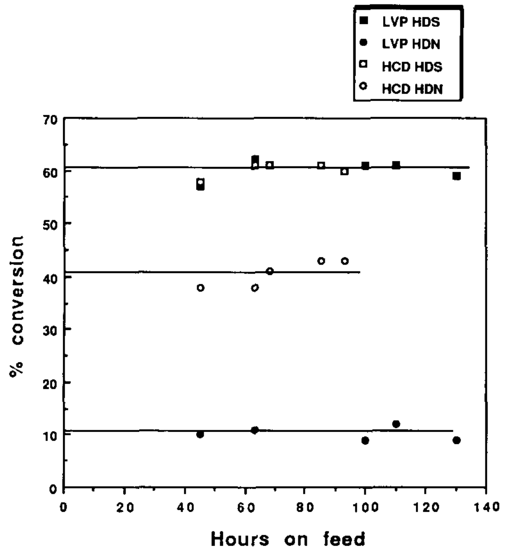

FIG. 5. Activity maintenance of LVP and HCD catalysts in the hydroprocessing of HCCO feed.

concentration. The overall HDS activities of both unpromoted and promoted catalysts are lowered by a factor of 10–15 in the presence of nitrogen-containing species. Nevertheless, the increase in HDS activity upon promotion is still about 13-fold, much the same as that observed in the neat DBT experiment. These observations suggest that the intrinsic HDS activity of the $Co_2(CO)_8$ promoted catalytic sites is the same with or without N compounds present, that adsorption of N compounds blocks HDS (*27*), and that the promoted sites have adsorption properties essentially the same as unpromoted MoS_2 sites. On the other hand, activities for HDN show relatively small increases corresponding to a promotion factor of ~1.7. Since no promotion of HDN was observed for Co-treated bulk MoS_2, we suspect that even this small promotion factor observed for the supported materials is the result of morphological changes rather than an electronic effect. Finally, it should be pointed out that both HDS and HDN activities level off when the Co/Mo ratio exceeds 0.2. Conventional promotion techniques reported in the literature typically show an optimum promotion at Co/Mo atomic ratios ~0.33 or higher. Clearly, the LVP method using $Co_2(CO)_8$ makes more effective use of the promoter metal.

Figure 5 compares the results obtained for the Co/MoS/AlS-B catalyst and the commercial catalyst HCD in the hydroprocessing of HCCO feed carried out in the CSTR unit. The percentage removal of sulfur and nitrogen, plotted as a function of time-on-stream, clearly indicates that the two catalysts have similar activity maintenance. However, the LVP catalyst exhibits a very high selectivity for HDS. Table 5

TABLE 5

HDS/HDN Selectivity and Activity on Real Feeds

Feed	Catalyst	% Mo	k_{HDS}	k_{HDN}	S_{HDS}
HCCO[a]	Co/MoS/AlS	—	2.0	10.8	0.19
	HCD	—	2.0	42.6	0.05
Gas oil[b]	Co/MoS/AlL-B	3.1	1.17	0.23	5.1
	Co/MoS/AlL-A	9.5	2.30	0.33	6.7
	Co/MoS/AlS-J	9.3	2.13	0.36	5.9
	Co/MoS/AlS-K	13.8	1.68	0.28	6.0
	KF840	—	1.68	0.45	3.7

[a] Conditions: CSTR, 3.15 MPa, 325°C, 1.0 LHSV, 3000 S/B.

[b] Conditions: Fixed bed, 7.3 MPa, 360°C, 1.0 LHSV.

TABLE 6

Activities of Various Promoted Catalysts for DBT HDS and THQ HDN

Promoter	Relative activity[a]		Promotion factor		HDS/HDN
	HDS	HDN	HDS	HDN	
None	1.0	2.7			0.37
$Co^{II}(NO_3)_2$	5.8	5.6	5.8	2.1	1.0
$Co^{II}(S\Phi)_4^{2-}$	5.4	1.0	5.4	0.4	5.4
$Co_2(CO)_8$	13.0	4.9	13.0	1.8	2.7
$Ni^0(P\Phi_3)_2(CO)_2$	16.0	6.0	16.0	2.2	2.7
Ni^0(COD)	14.3	5.2	14.3	1.9	2.7
Fe^0(COD)(Tol)	1.1	1.5	1.1	0.6	0.7

Note. Reaction conditions: Batch reactor, 0.8 wt% S as DBT + 0.8 wt% N as THQ/decalin, 1 g catalyst, 350°C.

[a] Activities are normalized to the HDS activity of the nonpromoted catalyst.

gives a more quantitative comparison of the activities and selectivities of these two catalysts in the hydrotreating of the HCCO feed and the gas oil. The LVP catalyst is at least as active as the commercial catalysts (HCD and KF840) for HDS. In contrast, its activity for HDN is lower by a factor 2 to 4 resulting in the high HDS selectivity.

Note that both HDS and HDN volumetric activities obtained in the gasoil runs are seen to pass through a maximum with increasing Mo loading. This most likely reflects the formation of large crystallites of MoS_2 on the alumina support.

Other Promoters

In addition to the work on $Co_2(CO)_8$ promotion, we briefly investigated the use of several other promoter species with MoS_2 on alumina. Two Co^{II} promoters were tested for comparison with the low-valent $Co_2(CO)_8$: conventional $Co(NO_3)_2$ and $Co(SPh)_4^{2-}$. Two low valent Ni^0 complexes and one low-valent iron (Fe^0) complex were also studied. Note that low-valent Ni in the form of $Ni(CO)_4$ was previously used by Angulo *et al.* (*18*). Table 6 summarizes the activities of these catalysts for HDS and HDN using the DBT/1,4-THQ model feed in the semi-batch autoclave reactor. All the catalysts listed in the table have promoter/Mo ratios above the value at which the activities of the Co-LVP catalysts level off. In general, the low-valent Ni and Co promoters are the most effective for HDS, with promotion factors between 13 and 16. For the Co^{II} species, promotion ratios of 5.6 were obtained, while no HDS promotion was observed with the low-valent Fe treatment. The HDN activity values of 5–6 correspond to a promotion factor of ~2 in all cases except $Co(SPh)_4^{2-}$ and Fe^0. The latter two species actually led to decreased HDN activity. Note that Ni offers no significant advantage over Co in either HDS or HDN.

Nature of the Promotion

Current ideas of promotion focus on the specific structure of the Co/Mo/S ensemble in the "zone of contact" or interface (Fig. 1). Many competing hypotheses have been proposed for this specific structure. All of the models, whether for supported or unsupported catalysts, suffer from the same problem, i.e., the lack of precise knowledge of the degree of MoS_2 dispersion and/or Co concentration at the interface. It is the same problem which is at the source of the confusion in the literature regarding the nature of promotion. There are two basic concepts: first, "electronic promotion," meaning that Co and Mo act together to create sites or vacancies that are more active than sites on either single component (pseudo-binary). The second concept, "structural promotion," refers to a Co/Mo interaction which increases the dispersion of either phase, thus increasing activity. In the later idea, either the dispersion of MoS_2 is increased or MoS_2 is dispersing a very active form of Co. Our results on bulk Mo/S suggest that both electronic and structural promotion coexist. The structural promotion is dependent upon the capacity of the particular unpromoted Mo/S system to undergo morphological changes during the promotion process: amorphous materials being more amenable

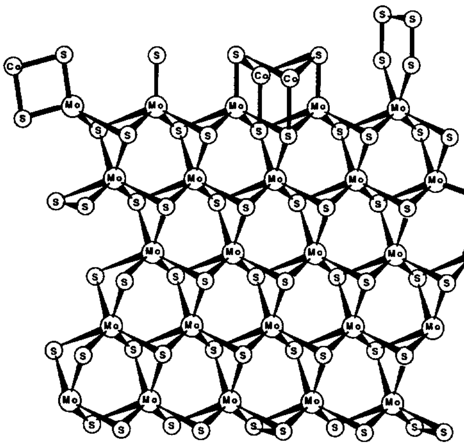

FIG. 6. Possible structures for a promoted molybdenum sulfide edge site.

to structural changes than crystalline materials. The electronic promotion factor is common to all morphologies of the Mo/S systems and is best estimated when the structural promotion is minimum, i.e., when measured on crystalline MoS_2. The electronic factor of Co is 3.3 (upper limit) while the structural factor lies between 0 and 4.3 (crystalline MoS_2 and alumina-supported MoS_2, respectively).

Finally, the chemistry involved in the synthesis of the covalent Co/Mo/S clusters suggests some possible local structures that can be formed upon reaction of the edges with low-valent promoters. A quick analysis of the possible structures existing at the edges of a MoS_2 layer, points out striking similarities with the MoS_4^{2-}, $Mo_2S_4(S_2)_2^{2-}$, and $Mo_3S_3^{2-}$ species. Figure 6 illustrates a speculative possibility for the Co/Mo structures on the edge of the layer. It is interesting to note that the environment of the Co can be either tetrahedral or octahedral, depending upon the number of sulfur ligands required to stabilize such atoms at the edge of MoS_2. In view of the low-temperature chemistry involved in LVP and the occurrence of significant rearrangements of the edge surfaces at the reaction temperature, it is not clear to us whether one of the two environments, if relevant, is a representative model of the structure of the catalytic sites. In this regard, it is relevant to mention the results of two recent studies. Clausen *et al.* (*36*) and Louwers Prins (*37*) both suggested that the environment of the Co and/or Ni in the catalysts is rather square pyramidal and most likely situated above the square faces of the MoS_6 trigonal prisms along the edges of the crystallites. These findings were based on EXAFS and XANES Co and/or Ni K-edge spectra. Ledoux *et al.* (*38*) identified by Co NMR two new types of Co species, called "distorted tetrahedral Co" and "rapid octahedral Co." They suggested that the square pyramidal structure would be the "rapid octahedral Co."

CONCLUSIONS

A synthesis of novel hydrotreating catalysts has been achieved by using the low-valent promotion technique. When applied to supported or preformed bulk molybdenum sulfides, a wide range of promotion factors were observed. The promotion factors are likely to be both electronic and structural in nature. The catalysts prepared by the LVP method are active for both HDS and HDN. Moreover, they exhibit an unusually high selectivity for HDS.

REFERENCES

1. Lipsch, J. M. J. G., and Schuit, G. C. A., *J. Catal.* **15,** 179 (1969).

2. Massoth, F. E., *in* "Advances in Catalysis" (D. D. Eley, H. Pines, and P. B. Weisz, Eds.), Vol. 27, p. 265. Academic Press, New York, 1978.

3. Delmon, B., *in* "Proceedings, Climax 3rd International Conference on Chemistry and Uses of Molybdenum" (H. F. Barry and P. C. H. Mitchell, Eds.), p. 73. Climax Molybdenum Co., Ann Arbor, Michigan, 1979.

4. Voorhoeve, R. S. H., and Stuiver, J. C. M., *J. Catal.* **23,** 228 (1971).

5. Farragher, A. L., and Cossee, P., *in* "Proceedings, 5th International Congress on Catalysis, Palm Beach, 1972" (J. W. Hightower, Ed.), p. 1301. North-Holland, Amsterdam, 1973.

6. Ratnasamy, P., and Sivasanker, S., *Catal. Rev.-Sci. Eng.* **22,** 401 (1980).

7. Topsøe, H., Clausen, B. S., Candia, R., Wivel, C., and Mørup, S., *J. Catal.* **68,** 433 (1981).

8. Ho, T. C., Young, A. R., Jacobson, A. J., and Chianelli, R. R., U.S. Patent No. 4,591,429 (1986).

9. Gatsis, J. G., U.S. Patent No. 3,249,556 (1966); U.S. Patent No. 3,331,769 (1967).

10. Bearden, R., and Aldridge, C. L., U.S. Patent No. 4,134,825 (1979).

11. Ho, T. C., and McCandlish, L. E., U.S. Patent No. 4,595,672 (1986).

12. Pan, W. H., McKenna, S. T., Chianelli, R. R., Halbert, T. R., Hutchings, H. H., and Stiefel, E. I., *Inorg. Chim. Acta* **97,** L17 (1985).

13. Stiefel, E. I., Pan, W. H., Chainelli, R. R., and Ho, T. C., U.S. Patent No. 4,581,125 (1986).

14. Eltzner, W., Breysse, M., Lacroix, M., and Vrinat, M., *Polyhedron* **5,** 203 (1986).

15. Eltzner, W., Breysse, M., Lacroix, M., Leclercq, C., Vrinat, M., Muller, A., and Diemannn, E., *Polyhedron* **7,** 2405 (1988).

16. Curtis, M. D., Penner-Hahn, J. E., Schwank, J., Barralt, O., McCabe, D. J., Thompson, L., and Waldo, G., *Polyhedron* **1,** 2411 (1988).

17. Halbert, T. R., Stiefel, E. I., Chianelli, R. R., and Ho, T. C., U.S. Patent No. 4,839,326 (1989).

18. Angulo, M., Mauge, F., Duchet, J. C., and Lavalley, J. C., *Bull. Soc. Chim. Belg.* **96,** 925 (1987).

19. Stiefel, E. I., Halbert, T. R., Coyle, C. L., Pan, W. H., Ho, T. C., Chianelli, R. R., and Daage, M., *Polyhedron* **8,** 1625 (1989).

20. Wolff, T., Berg, J., Hodgson, K., Frankel, R., and Holm, R., *J. Am. Chem. Soc.* **101,** 4140 (1979).

21. Halbert, T. R., Cohen, S. A., and Stiefel, E. I., *Organometallics* **4,** 1689 (1985).

22. Jacobson, A. J., Chianelli, R. R., and Whittingham, M. S., *in* "Proceedings, Climax Molybdenum," pp. 209–212, 1979.

23. Roxlo, C. R., Daage, M., Ruppert, A. F., and Chianelli, R. R., *J. Catal.* **100,** 176 (1986).

24. Seiver, R. L., and Chianelli, R. R., U.S. Patent No. 4,540, 482 (1985); U.S. Patent No. 4,544,481 (1985).

25. Vrinat, M. L., *Appl. Catal.* **6,** 137 (1983).

26. Ho, T. C., and Sobel, J. E., *J. Catal.,* **128,** 581 (1991).

27. Ho, T. C., *Catal. Rev.-Sci. Eng.* **30,** 117 (1988).

28. Ho, T. C., White, B. S., and Hu, R., *AIChE J.* **36,** 685 (1990).

29. van Dongen, R. H., Bode, D., and van der Eljk, H., and van Klinken, J., *Ind. Eng. Chem. Proc. Des. Dev.* **19,** 630 (1980).

30. Muller, A., Diemann, E., Jostes, R., and Bogge, H., *Angew. Chem. Int. Ed.* **20,** 934 (1981).

31. Topsøe, H., *in* "Surface Properties and Catalysis by Non-Metals," (J. P. Bonnelle, Ed.), pp. 329–360. Reidel, New York, 1983.

32. Chianelli, R. R., *Int. Rev. Phys. Chem.* **2,** 127 (1982).

33. Chianelli, R. R., Ruppert, A. F., Behal, S. K., Kear, B. H., Wold, A., and Kershaw, R., *J. Catal.* **92,** 56 (1985).

34. Harris, S., and Chianelli, R. R., *J. Catal.* **98,** 17 (1986).

35. Schneider, R. L., Howe, R. F., and Watters, K. L., *Inorg. Chem.* **23,** 4593 (1984).

36. Clausen, B. S., Niemann, W., Zeuthen, P., and Topsøe, H., *in* "ABS.ACS, 199th National Meeting, Boston, 1990," pp. 208.

37. Louwers, S. P. A., and Prins, R., *in* "ABS.ACS, 199th National Meeting, Boston, 1990," pp. 211.

38. Ledoux, M. J., Michaux, O., Agostini, G., and Pannissod, P., *J. Catal.* **102,** 275 (1986).